Exp Brain Res
DOI 10.1007/s00221-012-3226-1

RESEARCH ARTICLE

Electrocorticographic (ECoG) correlates of human arm movements

Nicholas R. Anderson · Tim Blakely · Gerwin Schalk · Eric C. Leuthardt · Daniel W. Moran

Received: 23 November 2011 / Accepted: 8 August 2012

Abstract Invasive and non-invasive brain–computer interface (BCI) studies have long focused on the motor cortex for kinematic control of artificial devices. Most of these studies have used single-neuron recordings or electroencephalography (EEG). Electrocorticography (ECoG) is a relatively new recording modality in BCI research that has primarily been built on successes in EEG recordings. We built on prior experiments related to single-neuron recording and quantitatively compare the extent to which different brain regions reflect kinematic tuning parameters of hand speed, direction, and velocity in both a reaching and tracing task in humans. Hand and arm movement experiments using ECoG have shown positive results before, but the tasks were not designed to tease out which kinematics are encoded. In non-human primates, the relationships among these kinematics have been more carefully documented, and we sought to begin elucidating that relationship in humans using ECoG. The largest modulation in ECoG activity for direction, speed, and velocity representation was found in the primary motor cortex. We also found consistent cosine tuning across both tasks, to hand direction and velocity in the high gamma band (70–160 Hz). Thus, the results of this study clarify the neural substrates involved in encoding aspects of motor preparation and execution and confirm the important role of the motor cortex in BCI applications.

Keywords Electrocorticography · Subdural electroencephalography · Motor cortex · Brain–computer interfaces · Arm tuning · Cosine tuning

N. R. Anderson (✉)
Department of Biomedical Engineering, Cortech Solutions and Washington University in Saint Louis, 1409 Audubon Blvd, Wilmington, NC 28403, USA
e-mail: NickR.Anderson@gmail.com

T. Blakely
Department of Computer Science and Engineering, Washington University in Saint Louis, 1815 E Calhoun, Seattle, WA 98112, USA

G. Schalk
Wadsworth Center, C650 Empire State Plaza, Albany, NY 12201, USA

E. C. Leuthardt
School of Neurosurgery and Department of Biomedical Engineering, Washington University in Saint Louis, 660 S. Euclid Avenue, Campus Box 8057, St. Louis, MO 63110, USA

D. W. Moran
Department of Biomedical Engineering, Washington University in Saint Louis, 300F Whitaker Hall, Campus Box 1097, St. Louis, MO 63021, USA

Introduction

Over the past several decades, neurophysiologists and biomedical engineers have applied significant effort toward creating useful brain–computer interface (BCI) systems for the impaired (Dobelle et al. 1973; Bullara et al. 1979; Wolpaw et al. 2002). During this same period, our ability to collect, process, and understand brain signals has increased substantially (Schwartz et al. 2006). Because of these efforts, BCIs based on electroencephalography (EEG) have already been installed in the homes of a few impaired individuals (Kubler et al. 2005; Nijboer et al. 2008; Klobassa et al. 2009). For these patients, BCI devices restore the capacity to interact with the world again. EEG is widely used for research and development because it is safe, inexpensive, and effective (Wolpaw and Birbaumer 2005); however, EEG can only detect synchronous changes

Published online: 22 September 2012

in large areas of cortex (Nunez and Srinivasan 2006), thus placing significant limitations on EEG devices in terms of providing finer degrees of device control to a patient.

Results from prior studies based on implanted microelectrodes primarily in non-human primates show that the scope of recordings from individual neurons is the converse of EEG recordings (Bullara et al. 1979; Georgopoulos et al. 1982). Single-unit recordings have performed successfully in device control experiments in the laboratory (Moran and Schwartz 1999a, b; Georgopoulos et al. 1982; Schwartz et al. 1988; Wang et al. 2007, 2010), enabling closed-loop control of a computer cursor (Serruya et al. 2002; Taylor et al. 2002) and even a robotic arm (Velliste et al. 2008). At the same time, despite isolated encouraging successes in clinical applications of these methods (Hochberg et al. 2006), single-unit recordings have yielded limited success outside of the laboratory setting, mainly due to unsolved problems with the long-term robustness of the recorded signals (Baker et al. 1999; Liu et al. 1999; Blake et al. 2010; Retterer et al. 2008).

The limitations of both signal acquisition techniques described above have led to the exploration of local field potential (LFP) recordings and a similar recording modality (electrocorticography [ECoG]), closely related technologies that record signals from populations of neurons (Leuthardt et al. 2006b; Schwartz et al. 2006). ECoG has had successes showing that it contains more information than EEG, but there are only preliminary findings to address stability issues seen with single units (Chao et al. 2010). Early successes using ECoG were based on approaches developed for EEG. These approaches make use of brain signal correlates of gross motor movements (e.g., moving a hand vs. rest) and equivalent motor imagery. While these approaches provide robust ECoG signals that can support good BCI performance, such BCI performance depends on non-intuitive imagery and thus may be suboptimal (Miller et al. 2007; Leuthardt et al. 2006a). A number of recent studies have shown that ECoG signals from the motor cortex in the 70–160-Hz range show strong encoding of actual and imagined motor activity (Wang et al. 2007; Schalk et al. 2007b; Pistohl et al. 2008; Sanchez et al. 2008; Kubanek et al. 2009). Similar ECoG activations have been successfully used for one- and two-dimensional BCI control in subjects with epilepsy (Leuthardt et al. 2004; Schalk et al. 2008). Given these successes in decoding gross movements and corresponding motor imagery, it is logical to further explore high-frequency (70–160-Hz range) ECoG signals for more precise encoding.

Recently, researchers have begun to explore the correlation between two-dimensional hand movements and ECoG recordings (Schalk et al. 2007b; Pistohl et al. 2008; Sanchez et al. 2008). These studies focused on one experiment and failed to explore the relationship between tracing and center-out reaching tasks that has been elucidated in non-human primates. Single-neuron approaches are usually employed to decode directional tuning and other movement parameters such as speed. Studies have shown that firing rates of single units in the primary motor cortex can be highly correlated with arm kinematics such as position, direction, speed, and velocity (Moran and Schwartz 1999a, b; Georgopoulos et al. 1982; Schwartz et al. 1988; Wang et al. 2007, 2010), and a direction and velocity signal-based BCI has been successfully implemented (Serruya et al. 2002; Taylor et al. 2002; Velliste et al. 2008). We have previously shown that single-unit firing rates correlate well with high frequencies of local field potentials and exhibit tuning to movement kinematics (Heldman et al. 2006). Thus, the aim of this study is to better characterize the differential ECoG signals encoded by hand direction, velocity, and speed.

Methods

Cortical activity model

This study investigated the cortical representation of ECoG signals for two-dimensional hand position and velocity in humans. This model was adapted from the model used in the previous primate studies (Wang et al. 2007; Moran and Schwartz 1999a, b). Our hypothesis was that the relationship between motor cortical ECoG activity and hand kinematics can be described by:

$$A(t) = b_0 + b_s\left\|\vec{V}(t)\right\| + \vec{B}_v \cdot \vec{V}(t) + \vec{B}_p \cdot \vec{P}(t) \quad (1)$$

where $A(t)$ is the instantaneous ECoG spectral amplitude of a given frequency band at any time t, b_0 is the baseline activity of a feature, and b_s is the portion of the feature activity modulated by hand speed. The remaining variables are all two-dimensional vectors, that is, B_v, B_p, $V(t)$ and $P(t)$. B_v is the preferred direction (PD) of a specific feature, and B_p is the preferred gradient (PG) of the same feature. Preferred gradient varies with the magnitude of displacement from the central location. $V(t)$ and $P(t)$ are the hand velocity and hand position, respectively. The magnitudes of B_p and B_v represent the depth of modulation for each tuning curve (position and velocity), respectively. The depth of modulation is determined by the magnitude of the resulting b_x and b_y, specifically DoM $= \|[b_x, b_y]\|$. Equation 1 is based on the neuronal activity model proposed by Moran and Schwartz (1999a).

Equation 1 can be broken into the following Eqs. 2–5 for analysis in order to calculate the portion of the signal encoded by each of the kinematic components independently. We analyzed three kinematic components during

the movement period for their relative depths of modulation and statistical significance. We used four equations to model the kinematic components of position (Eqs. 2), direction (Eq. 3), speed (Eq. 4), and velocity (Eq. 5):

$$\bar{A} = b_0 + b_{px}\bar{x} + b_{py}\bar{y} \quad (2)$$

$$\bar{A} = b_0 + b_{\mathrm{dx}}\frac{\bar{\dot{x}}}{\bar{s}} + b_{\mathrm{dy}}\frac{\bar{\dot{y}}}{\bar{s}} \quad (3)$$

$$\bar{A} = b_0 + b_s\bar{s} \quad (4)$$

$$\bar{A} = b_0 + b_{vx}\bar{\dot{x}} + b_{vy}\bar{\dot{y}} \quad (5)$$

In Eqs. 2–5, $\bar{A}$ is the average spectral amplitude deviation from baseline of the ECoG data over a given time period in a given frequency band, and $\bar{x}$ and $\bar{y}$ represent average hand position in that same time period (mapped from screen positions). Similarly, $\bar{\dot{x}}$ and $\bar{\dot{y}}$ represent average hand velocity from the same time period as $\bar{A}$. Mean speed during a given time period, denoted $\bar{s}$, is used to calculate direction in Eq. 3 as well as speed modulation in Eq. 4. The feature's baseline amplitude is b_0; other variables, b_{px}, b_{py}, b_{dx}, b_{dy}, b_{vx}, and b_{vy}, are the values of the preferred directions/gradients calculated from their associated components.

A is calculated as the percent deviation from a baseline wherein the task-dependent baseline was subtracted from the signal of interest and then the resulting signal was divided by the baseline value. Similarly, the movement kinematics are standardized as ratios of the maximum in order to normalize the variables between 1 and −1. Equation 2 is a model for position and regresses the deviation from baseline amplitude in signal ($\bar{A}$) to the mean position of the cursor. Similarly, for Eq. 3, the variable A is regressed to the horizontal and vertical directions of the cursor movements. Equation 4 is used for speed tuning and only has one component, s, which is the magnitude of the derivative of both the $\bar{x}$ and $\bar{y}$ positions. By combining speed and direction, Eq. 5 models velocity, and the two vectors $\dot{x}$ and $\dot{y}$ represent the corresponding cursor movement velocities.

Subjects and data collection

Our study included seven patients with epilepsy who underwent clinical subdural ECoG monitoring for seizure localization. The study was approved by the Washington University Institutional Review Board, and all subjects provided informed consent. Subject information is shown in Table 1.

The subjects performed two different tasks using a Microsoft Sidewinder II force feedback joystick that was placed at a comfortable distance in order to allow for the desired range of arm movements. The joystick was placed at chest height on a table in front of each subject such that he or she could comfortably grasp it using the hand that was contralateral to the implanted electrodes. Subjects used their hands and arms to manipulate the joystick in open-loop experiments as described below. Joystick movements involved both the arm and wrist because of the force involved and displacement required. These movements activated multiple muscle groups, making the experiments less specific but more likely to yield results at the level recorded by ECoG. This joystick had a force feedback feature that provided a linear centering force of 4.5 Newtons at the top of the joystick when displaced from the center and provided an equivalent force resisting circular motion. Visual feedback for the experiments was displayed on a computer monitor that was placed approximately 18 in. from the subjects.

Data were collected by splitting the ECoG signals from the subjects to allow both research and clinical recordings simultaneously. FDA-approved amplifiers (i.e., USBamp, Guger Technologies, Graz, Austria) were used to record the signals for research purposes. Data were collected at a sampling rate of 1,200 Hz (bandpass 0.5–500 Hz), similar to the settings used in the previous work (Wisneski et al. 2008). Data acquisition and stimulus presentation were accomplished using the BCI2000 software package (Schalk et al. 2004) with custom experimental paradigms.

Table 1 These experiments were run on seven epilepsy subjects with normal cognition

Sex	Handed	Age	Cognition	Hand used	Elec CO	Elec T	Location
Male	Left	14	Normal	Right	12	16	PM,M,S
Female	Right	27	Normal	Left	24	24	PM,M,FEF,T,PFC
Female	Right	46	Normal	Left	42	42	PM,M,S,FEF,T,PFC
Female	Right	9	Normal	Left	46	46	PM,M,S,FEF,T,PFC
Male	Right	43	Normal	Right	36	36	PM,M,S,T,PFC
Female	Right	16	Normal	Right	56	0	PM,M,S,FEF,T,PFC
Female	Right	48	Normal	Right	11	11	PM,M,FEF,T,

Different numbers of electrodes were run on some patients for center-out (CO) and tracing (T). The location information has the same areas as Fig. 4 prefrontal (PFC), frontal eye fields (FEF), temporal (T), somato-sensory (S), motor (M), premotor (PM)

Experimental paradigms

We designed two tasks to dissociate position and direction kinematics from each other. The first task was a classic center-out reaching task, first proposed by Georgopoulos et al. (1982). The second task was based on the circular drawing task first designed by Moran and Schwartz to dissociate position from velocity (Wang et al. 2007; Moran and Schwartz 1999a, b). Data were collected from seven subjects for the center-out reaching task and six subjects for the tracing task; one subject was not able to perform both tasks.

In the center-out task, the subject moved a cursor from the center of the screen to a random target placed toward the periphery of the screen. The task specifics are described below and are also outlined in Fig. 1. The first period was a delay before a goal target was presented to the subject (baseline period; 300 ms). Signals during this period were used as a baseline in the analyses. The goal target then briefly changed color (target-encoding period; 300–500 ms) to indicate that it was the desired target in this trial. Another delay (delay period; 300 ms) followed the target-encoding period. Subjects then used the joystick to move the cursor to the appropriate target (movement period; 500–3,000 ms), which was the period of interest to analyze the kinematic components in question. Upon reaching the target, the subject had to hold the cursor over the target for a length of time (hold period; 300–500 ms). A reward period followed wherein the desired target turned green if the trial was completed correctly, or red if the trial was completed incorrectly. To complete the cycle for the task, the cursor was re-centered by the computer, and the joystick was re-centered by the subject so that each trial began in the same location. The targets each were presented in a pseudo-randomized order 10 times for a total of 80 movements per subject.

The tracing task was based on a drawing task used in prior studies (Moran and Schwartz 1999b; Schwartz and Moran 1999). In this paradigm, the subject's task was to trace the path of a computer-controlled arrow (blue) with a subject-controlled cursor arrow (red) using the joystick (see Fig. 1). The direction of rotation of the arrow changed between trials (i.e., clockwise or counterclockwise), so that velocity encoding could be dissociated from position encoding. The subject was instructed to match the length and direction of the computer-generated arrow with his or

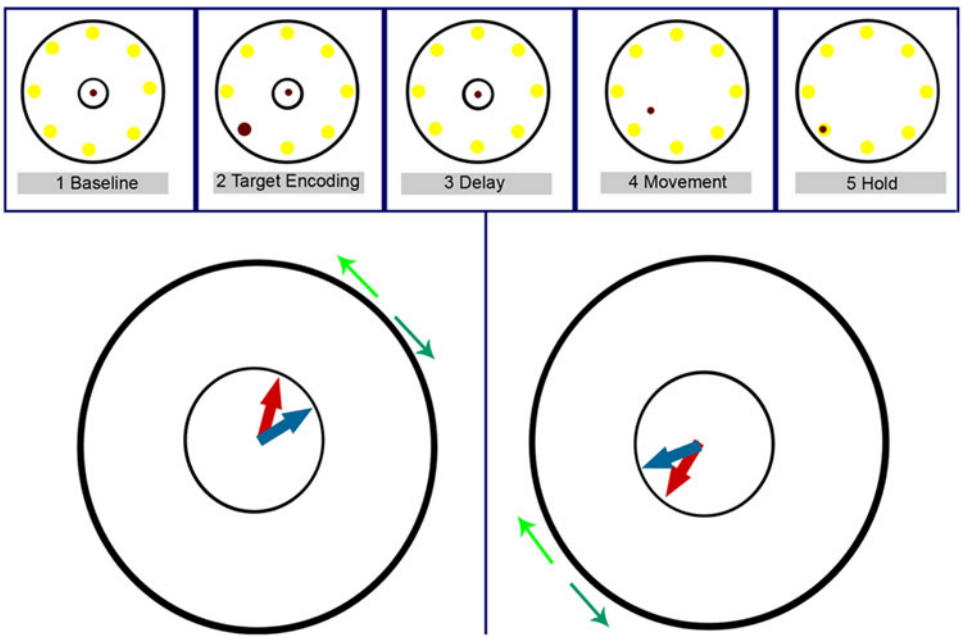

Fig. 1 The center-out and arrow tracing tasks. *Top* The center-out task as performed in this study. There were 5 different key periods to the task. A baseline was collected while the subject centered the cursor in the middle of the screen (i.e., no force/displacement applied to joystick). The target was then displayed for 300–500 ms by changing the color of the "correct" target. A 300-ms delay period followed the target-encoding period, wherein the target cueing was extinguished, and the subject had to hold the correct target location in memory. At the end of the delay period, a ring in the center of the display disappears as a "go signal" to the subject and then moves to the appropriate target. Once the subject reaches the target, they have to hold the cursor on the target for a period of time (300 ms). *Bottom* The *arrow* tracing task was performed by having the subject match the radius of the *blue arrow* with the *red arrow* and the push the *blue arrow* around the *circle* in the direction the computer would allow. Both clockwise and counter-clockwise conditions were run on this task in order to dissociate position and direction of movement. The task was also run with two different radii; however, the results from both radii were combined in the final analyses (color figure online)

her cursor-controlled arrow using the joystick. The computer-generated arrow was 2.5 or 5 cm long and was centered in the middle of the monitor. The arrow position and direction matched the joystick position and direction. Once the subject matched both the radius and angle of the blue cue arrow, the computer rotated the arrow either clockwise or counter clockwise, slightly ahead of the subject-controlled arrow. The subject controlled the overall rate of rotation (i.e., speed) by the rate at which it reacquired the rotated blue arrow. The subjects performed a total of at least 20 complete circle tracings over a 9-min period, five repetitions in each direction (clockwise or counter clockwise) for each radius (2.5 or 5 cm).

Performing the tracing task in two directions dissociated the movement kinematics of position and velocity, which are correlated in the center-out task since it uses straight-line movements. This dissociation is accomplished in the tracing task by requiring a subject to move his or her arms at opposite velocities in the same position and at the same velocity in opposite positions (demonstrated in Fig. 1). When the arrows are on opposite sides of the circle and are moving in opposite directions, the direction of movement kinematics is in the same direction along the circumference. The light green arrow represents the direction of movement for clockwise movement on the right and for counter-clockwise movement on the left, which in both cases is up and to the left.

Kinematics and analysis

All trials having movement periods lasting between 0.5 and 3 s were accepted for the center-out task. Approximately 80 trials for both tasks conformed to these standards. Short trials (i.e., <0.5 s) were excluded because they included movements that were initiated during the delay period. Data for the tracing task were accepted if a subject moved in the same direction for at least 300 ms while within 2.5 mm of the given radius (e.g., 2.5 or 5 cm). After applying these criteria, our data set included every subject and at least 75 trials for each task. The movement kinematics were normalized by averaging over the entire movement period.

Prior to performing our analyses, we applied notch filters (6 Hz wide, 3rd order Butterworth) centered at 60 Hz and its 2nd through 4th harmonics. We then performed power spectra calculations using the maximum entropy method (Press et al. 1992), as outlined in the previous work (Anderson et al. 2009). These spectra were created as estimations of power based on 100-ms sliding time windows and a model order of 30. A baseline was calculated during the first delay period for the center-out task and an average of all the data for the tracing task. Next, cosine tuning curves were fit on these spectra in 5-Hz bins using the cosine tuning Eqs. 3–5.

The tuning of the baseline activity normalized power in the spectra from 0 to 280 Hz in 5-Hz spectral bins was regressed to the normalized movement kinematics of the subject. Electrodes were divided up by Brodmann area, and tuning was calculated by regression to the models in Eqs. 2–5. The regression to each of the modeled kinetics was an attempt to demonstrate tuning and reject the null hypothesis that these models are not represented in the signals ECoG records. A specific channel and frequency band was considered statistically significant for this hypothesis when $p < 0.05$ for fit of regression to the model and depth of modulation (DOM) for this model was DOM > 5 % of baseline power. A specific channel was said to be tuned to the model and have statistical significance if at least one-third of the 70–160-Hz band of interest filled the criteria of statistical significance for a given band, in this case that would be at least any 6 of the 5-Hz bands in a given channel. The 6 bins needed to count a channel need not be continuous but would represent wideband tuning in the 70–160-Hz region. A specific Brodmann area was said to be statistically significant, have organized and not just spurious tuning, if the number of statistically significant channels in that Brodmann area exceeded the number expected by random chance at $p < 0.05$. Each feature (5-Hz frequency bin on each channel) was modeled to the direction, speed, and velocity of the joystick movements.

We considered two different statistics of tuning: mean depth of modulation and number of channels. The mean depth of modulation was used since it provided an expected measure of modulation on an electrode within a Brodmann area and was only computed using statistically significant channels. Discerning the number of channels with significant activations allowed us to estimate the likelihood that a channel would be tuned if future electrodes were placed in that area.

We averaged the 70–160-Hz band data to create a gamma band average for the functional areas (Fig. 4). We combined Brodmann areas to represent functional areas as follows: Areas 11 and 47, prefrontal cortex; Areas 9, 46, and 8, frontal eye fields (FEF); Area 6, premotor cortex; Area 4, motor cortex; Areas 1, 2 and 3, somato-sensory (Sensory) cortices; and Areas 21 and 22, temporal lobe.

After the preferred directions were calculated for each feature, they were compared to their counterparts (same frequency and channel) if both were statistically significant across tracing and center-out tasks. To do so, we compared the angle between the tuning of the preferred direction of one condition and the tuning of the preferred direction of the other condition. This comparison aided in determining the stability of the preferred direction for a particular feature.

Results

Kinematic Figs. 2 and 3 illustrate the setups for these experiments. Figure 2 illustrates all of the kinematic data from Subject 1 used in later analysis. Mean time and variance to each of the eight targets were similar for the center-out task (see Fig. 3, left). The data for the tracing task were segmented into octants based on the center-out task target location before any additional analysis was performed (see corresponding movement times in Fig. 3, right). These times are similar except for the octant at 90°. Each trial started in the octant at 90°, and the higher variance reflects the time it took to arrive in the upper octant from the subject's previous position.

Table 2 shows the number of channels that are statistically significant for each of the functional areas. Results for velocity tuning show that electrodes located in the motor cortex were consistently statistically significant for both the center-out and tracing tasks. The frontal eye fields and premotor cortex show more dominant tuning for the tracing task than for the center-out task.

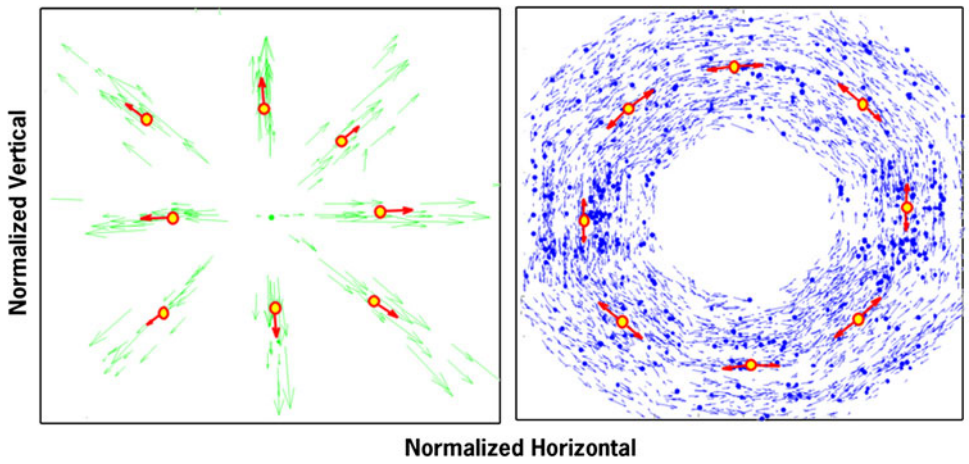

Fig. 2 Average kinematics for both the center-out and arrow tracing tasks. On the *left*: For the center-out task, the *green arrows* represent the average velocity of the cursor during a single movement. The *green arrows* are centered on the average position of the cursor during that same single movement. The *red arrows* are the mean velocities plotted at the mean position for each target (across all trials to that target). The mean velocity (*red*) *arrows* show approximately the same speed for any given direction. On the right: For the *Arrow* Tracing task, the *blue arrows* represent all the velocities used to create average values for the regression. The *red arrows* are the mean velocity all originating from the mean position in that octant. There are two mean velocity arrows for each position since the task was run in both the clockwise and counter-clockwise direction. This task showed fairly uniform velocity distributions like the center-out task (color figure online)

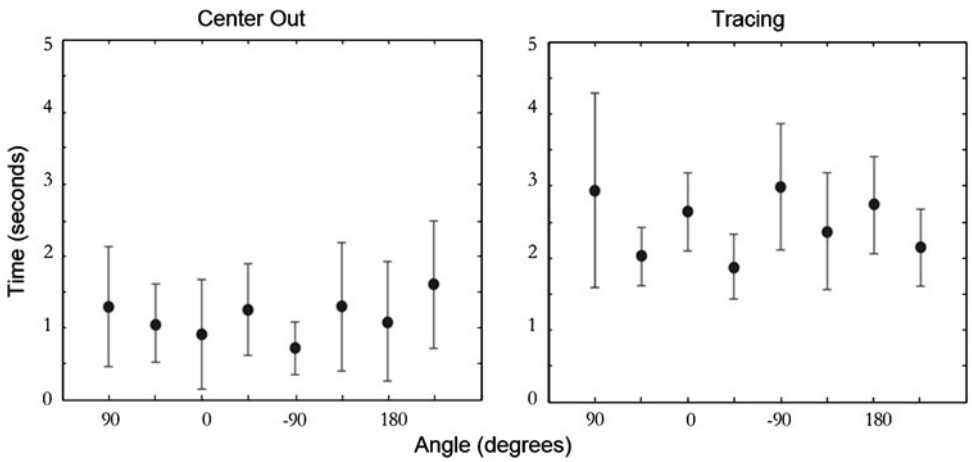

Fig. 3 Mean movement times and variance for trials in center-out task or time spent in a particular octant for the *Arrow* tracing task. The *black circles* represent the mean time spent in each of the conditions and the lines are one standard deviation above or below this mean. For the center-out task, the means were relatively consistent around 1.25 s, and variances were relatively consistent across locations. This was consistent with the similar velocities displayed in Fig. 2. For the tracing task, the average time spent in each octant was relatively consistent around 2–3 s. The variances on this were generally consistent with the exception of the octant located at 90°. Each trial started at 90° and the larger variability of time at this location is the result of the variable delay at the beginning of each trial

Table 2 Statistically significant electrodes from center-out and arrow tracing tasks across all parameters

Area	Prefrontal	FEF	Premotor	Motor	Somatosensory	Temporal
Center-out						
Electrodes	22	58	46	43	21	39
Direction	0	0	2	8*	1	0
Velocity	0	1	2	12*	2*	1
Speed	1	1	3*	3*	3*	0
Tracing						
Electrodes	16	39	32	34	15	39
Direction	0	3*	7*	4*	0	1
Velocity	0	4*	6*	3*	0	1

Electrodes were said to be statistically significant if they had at least 30 Hz of tuning in the bandwidth between 70 and 160 Hz. The regions that showed statistical significance were primarily located in the motor areas. Premotor and frontal eye fields (FEF) are more involved in the tracing task than the center-out task

* Statistical significance for the population

Figure 4 shows the tuning for each of the functional areas described earlier. The horizontal axis of each plot shows the functional areas, and the vertical axis shows the mean depth of modulation. Each of these plots shows the depth of modulation for each of the three kinematic components: direction, speed, and velocity. The results displayed are all statistically significant ($p < 0.05$) individually, but the motor cortical results show much larger depths of modulation for direction, speed, and velocity terms compared to the other functional areas.

Figure 5 illustrates the wideband tuning and inversion (low frequency tuned in the opposite direction compared to high frequency [>70 Hz]) that is prototypically seen in channels with strong ECoG tuning. Frequency is represented on the horizontal axes, and the vertical axes are a measurement of the modulation of that feature. The lengths of the tuning vectors in Fig. 5 are the depths of modulation

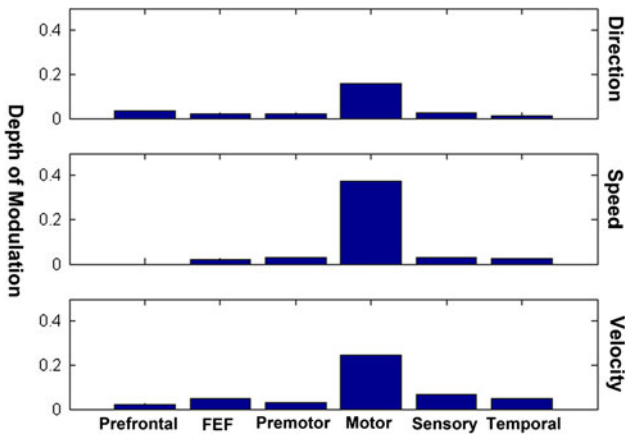

Fig. 4 Mean depth of modulation for each of the areas and the kinematic components involved in the center-out task. This is the mean depth of modulation for all statistically significant features from 70 to 160 Hz. Motor cortical areas show a much higher depth of modulation in this band than any other region

of each 5-Hz bin when compared to normalized movements, and the direction of the arrow is the modeled direction of the tuning. The 5-Hz bands with statistically significant tuning ($p < 0.05$) and depth of modulation (>5 %) are shown in red. The general direction of tuning and depth of modulation in given frequency bands is similar across the center-out and tracing tasks, and phase reversals are displayed between sub 50-Hz frequencies and 70–160-Hz frequencies tuning. There are also some differences across the tasks and to a lesser extent the direction and velocity results displayed: direction shows less depth of modulation than velocity that is consistent with velocity being tuned to a larger amount of the encoded information; the tuning in center-out is more consistent across bands than tracing likely because of the task design, specifically longer time windows available for center-out decoding.

Figure 6 quantifies the cross task stability of directional tuning across all the electrodes. As Fig. 5 showed for one example electrode, direction and velocity tuning of the neural substrates remains very stable across the center-out and tracing tasks. The angle between conditions is between 0 and 0.5 radians for the vast majority of the statistically tuned features. When the non-statistically significant depths of modulations were compared across these two tasks, they showed uniform distributions and did not remain stable. Similar features across both conditions for statistically significant depth of modulation indicate that there is stability in the kinematic tuning across both tasks.

Discussion

This study examined the kinematic tuning (i.e., direction, speed, and velocity) of cortical ECoG activations during joystick-based arm movements across different brain regions. The previous ECoG studies focused on motor

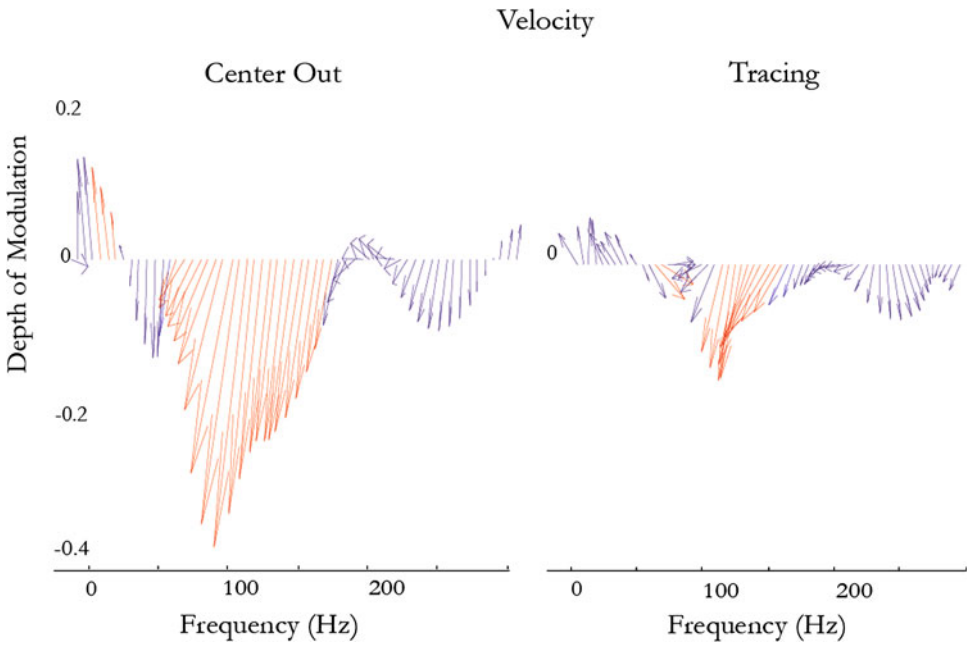

Fig. 5 Comparison of velocity tuning in 5-Hz bins for a single electrode in Brodmann area 4. The *arrows* indicate the two-dimensional direction of the tuning and length of the vector indicates the depth of modulation. *Red arrows* indicate statistical significance. This figure demonstrates the similarity in tuning for this electrode across tracing and center-out. This figure also demonstrates the wide gamma band tuning that occurs between approximately 70 and 60 Hz. Adjacent frequencies show similar tuning; however, there are small differences in adjacent bands that trend over frequency (color figure online)

areas without differentiating velocity, which has been shown to have stronger encoding from position during movements (Schalk et al. 2007a). Our experiments were based on the previous studies, and the results confirm those found in single-unit recordings in primates, where velocity and direction showed consistent strong tuning (Moran and Schwartz 1999b). The frequencies of interest are consistent with the previous ECoG literature that has shown that high gamma frequencies are most suitable for BCI and mapping applications (Miller et al. 2007, 2008; Crone et al. 1998).

The direction and velocity activations were modeled using a standard cosine tuning model that resulted in an array of preferred directions across the tested electrodes (Fig. 5). While individual electrodes showed more consistent preferred directions across the two tasks, cross electrode comparisons yielded a relatively uniform distribution, demonstrating that each electrode may have different, but stable tuning. The primary motor cortex, Brodmann Area 4, showed by far the best depth of modulation for the measured kinematics (Fig. 4); Area 4 also showed the most tuned electrodes in the center-out task. While our results showed the best tuning in Brodmann Area 4, it would be wise to cover adjoining areas as well in those with motor impairment and thus altered motor maps. Velocity is the primary kinematic used for BCI, and in this case, it has a high depth of modulation and the highest percentage of electrodes activated in the motor areas. This makes sense, since velocity is tuned to a larger share of the available information.

The previous studies have analyzed the angle of tuning with respect to the firing rates of individual neurons (Moran and Schwartz 1999a, b; Caminiti et al. 1990; Georgopoulos et al. 1989; Ganguly and Carmena 2009). The majority of these studies have indicated that the direction of this tuning changes for individual neurons; however, in ECoG, the tuning appears to be stationary over

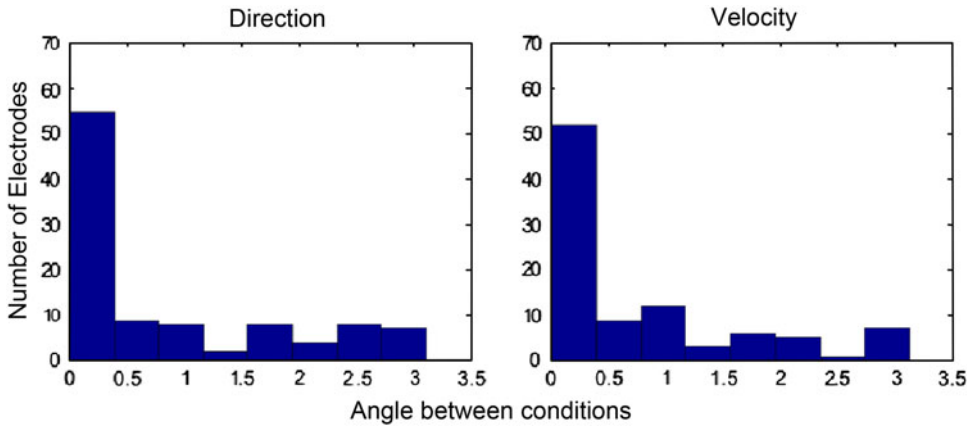

Fig. 6 Inter-task tuning. Preferred directions were calculated for each kinematic parameter during the *Arrow* tracing and center-out tasks. The figure above shows the average angle between preferred direction from the two tasks. The majority of statistically significant preferred directions show primarily small differences in tuning between the two tasks

time. The results shown in Figs. 5 and 6 characterize the robustness of this encoding across frequency and tasks. Additionally, Fig. 5 demonstrates that arm movement velocity is consistently encoded across large bandwidths (e.g., 70–160 Hz). In Fig. 6, both tasks exhibit primarily similar encoding for both direction and velocity. Combined with recent evidence of ECoG's long-term stability (Chao et al. 2010), these results suggest that motor cortical ECoG activity may be the optimal signal modality for long-term chronic BCI applications.

Acknowledgments This work was supported in part by the McDonnell Center for Higher Brain Function by grants from the NIH/NIBIB (EB006356 (GS) and EB000856 (GS)), and from the US Army Research Office (W911NF-07-1-0415 (GS), W911NF-08-1-0216 (GS)). N. Anderson was with Washington University in St. Louis and is now with Cortech Solutions. T. Blakely was with Washington University in St. Louis and is now with the University of Washington. G. Schalk is with the Wadsworth Center, Albany, NY. E. Leuthardt is with Washington University School of Medicine in St. Louis. D. Moran is with Washington University in St. Louis.

References

Anderson NR, Wisneski K, Eisenman L, Moran DW, Leuthardt EC, Krusienski DJ (2009) An offline evaluation of the autoregressive spectrum for electrocorticography. IEEE Trans Biomed Eng 56(3):913–916. doi:10.1109/TBME.2009.2009767

Baker SN, Philbin N, Spinks R, Pinches EM, Wolpert DM, MacManus DG, Pauluis Q, Lemon RN (1999) Multiple single unit recording in the cortex of monkeys using independently moveable microelectrodes. J Neurosci Methods 94(1):5–17

Blake AJ, Rodgers FC, Bassuener A, Hippensteel JA, Pearce TM, Pearce TR, Zarnowska ED, Pearce RA, Williams JC (2010) A microfluidic brain slice perfusion chamber for multisite recording using penetrating electrodes. J Neurosci Methods. doi:10.1016/j.jneumeth.2010.02.017

Bullara LA, Agnew WF, Yuen TG, Jacques S, Pudenz RH (1979) Evaluation of electrode array material for neural prostheses. Neurosurgery 5(6):681–686

Caminiti R, Johnson PB, Urbano A (1990) Making arm movements within different parts of space: dynamic aspects in the primate motor cortex. J Neurosci 10(7):2039–2058

Chao ZC, Nagasaka Y, Fujii N (2010) Long-term asynchronous decoding of arm motion using electrocorticographic signals in monkeys. Front Neuroeng 3:3. doi:10.3389/fneng.2010.00003

Crone NE, Miglioretti DL, Gordon B, Lesser RP (1998) Functional mapping of human sensorimotor cortex with electrocorticographic spectral analysis. II. Event-related synchronization in the gamma band. Brain 121(Pt 12):2301–2315

Dobelle WH, Stensaas SS, Mladejovsky MG, Smith JB (1973) A prosthesis for the deaf based on cortical stimulation. Ann Otol Rhinol Laryngol 82(4):445–463

Ganguly K, Carmena JM (2009) Emergence of a stable cortical map for neuroprosthetic control. PLoS Biol 7(7):e1000153. doi:10.1371/journal.pbio.1000153

Georgopoulos AP, Kalaska JF, Caminiti R, Massey JT (1982) On the relations between the direction of two-dimensional arm movements and cell discharge in primate motor cortex. J Neurosci 2(11):1527–1537

Georgopoulos A, Lurito J, Petrides M, Schwartz A, Massey J (1989) Mental rotation of the neuronal population vector. Science 243:234–236

Heldman DA, Wang W, Chan SS, Moran DW (2006) Local field potential spectral tuning in motor cortex during reaching. IEEE Trans Neural Syst Rehabil Eng 14(2):180–183

Hochberg LR, Serruya MD, Friehs GM, Mukand JA, Saleh M, Caplan AH, Branner A, Chen D, Penn RD, Donoghue JPD-n (2006) Neuronal ensemble control of prosthetic devices by a human with tetraplegia. Nature 442(7099):164–171

Klobassa DS, Vaughan TM, Brunner P, Schwartz NE, Wolpaw JR, Neuper C, Sellers EW (2009) Toward a high-throughput auditory P300-based brain-computer interface. Clin Neurophysiol 120(7):1252–1261. doi:10.1016/j.clinph.2009.04.019

Kubanek J, Miller KJ, Ojemann JG, Wolpaw JR, Schalk G (2009) Decoding flexion of individual fingers using electrocorticographic signals in humans. J Neural Eng 6(6):066001. doi:10.1088/1741-2560/6/6/066001

Kubler A, Nijboer F, Mellinger J, Vaughan TM, Pawelzik H, Schalk G, McFarland DJ, Birbaumer N, Wolpaw JR (2005) Patients with ALS can use sensorimotor rhythms to operate a brain-computer interface. Neurology 64(10):1775–1777. doi:10.1212/01.WNL.0000158616.43002.6D

Leuthardt EC, Schalk G, Wolpaw JR, Ojemann JG, Moran DW (2004) A brain-computer interface using electrocorticographic signals in humans. J Neural Eng 1(2):63–71

Leuthardt EC, Miller KJ, Schalk G, Rao RPN, Ojemann JG (2006a) Electrocorticography-based brain computer interface—The Seattle Experience. IEEE Trans Neural Syst Rehabil Eng 14(2):194–198

Leuthardt EC, Schalk G, Moran D, Ojemann JG (2006b) The emerging world of motor neuroprosthetics. A neurosurgical perspective. Neurosurgery 59(1):1–14

Liu X, McCreery DB, Carter RR, Bullara LA, Yuen TG, Agnew WF (1999) Stability of the interface between neural tissue and chronically implanted intracortical microelectrodes. IEEE Trans Rehabil Eng 7(3):315–326

Miller KJ, Leuthardt EC, Schalk G, Rao RP, Anderson NR, Moran DW, Miller JW, Ojemann JG (2007) Spectral changes in cortical surface potentials during motor movement. J Neurosci 27(9):2424–2432. doi:10.1523/JNEUROSCI.3886-06.2007

Miller KJ, Shenoy P, den Nijs M, Sorensen LB, Rao RN, Ojemann JG (2008) Beyond the gamma band: the role of high-frequency features in movement classification. IEEE Trans Biomed Eng 55(5):1634–1637. doi:10.1109/TBME.2008.918569

Moran DW, Schwartz AB (1999a) Motor cortical representation of speed and direction during reaching. J Neurophysiol 82(5):2676–2692

Moran DW, Schwartz AB (1999b) Motor cortical activity during drawing movements: population representation during spiral tracing. J Neurophysiol 82(5):2693–2704

Nijboer F, Sellers EW, Mellinger J, Jordan MA, Matuz T, Furdea A, Halder S, Mochty U, Krusienski DJ, Vaughan TM, Wolpaw JR, Birbaumer N, Kubler A (2008) A P300-based brain-computer interface for people with amyotrophic lateral sclerosis. Clin Neurophysiol 119(8):1909–1916. doi:10.1016/j.clinph.2008.03.034

Nunez PL, Srinivasan R (2006) Electric fields of the brain: The neurophysics of EEG, 2nd edn. Oxford University Press, Oxford

Pistohl T, Ball T, Schulze-Bonhage A, Aertsen A, Mehring C (2008) Prediction of arm movement trajectories from ECoG-recordings in humans. J Neurosci Methods 167(1):105–114. doi:10.1016/j.jneumeth.2007.10.001

Press WH, Teukolsky SA, Vetterling WT, Flannery BP (1992) Numerical Recipes in C

Retterer ST, Smith KL, Bjornsson CS, Turner JN, Isaacson MS, Shain W (2008) Constant pressure fluid infusion into rat neocortex from implantable microfluidic devices. J Neural Eng 5(4):385–391. doi:10.1088/1741-2560/5/4/003

Sanchez JC, Gunduz A, Carney PR, Principe JC (2008) Extraction and localization of mesoscopic motor control signals for human ECoG neuroprosthetics. J Neurosci Methods 167(1):63–81. doi:10.1016/j.jneumeth.2007.04.019

Schalk G, McFarland DJ, Hinterberger T, Birbaumer N, Wolpaw JR (2004) BCI2000: a general-purpose brain-computer interface (BCI) system. IEEE Trans Biomed Eng 51(6):1034–1043

Schalk G, Kubánek J, Miller KJ, Anderson NR, Leuthardt EC, Ojemann JG, Limbrick D, Moran D, Gerhardt LA, Wolpaw JR (2007a) Decoding two-dimensional movement trajectories using electrocorticographic signals in humans. J Neural Eng 4(3):264. doi: 10.1088/1741-2560/4/3/012

Schalk G, Kubanek J, Miller KJ, Anderson NR, Leuthardt EC, Ojemann JG, Limbrick D, Moran D, Gerhardt LA, Wolpaw JR (2007b) Decoding two-dimensional movement trajectories using electrocorticographic signals in humans. J Neural Eng 4(3):264–275. doi:10.1088/1741-2560/4/3/012

Schalk G, Miller KJ, Anderson NR, Wilson JA, Smyth MD, Ojemann JG, Moran DW, Wolpaw JR, Leuthardt EC (2008) Two-dimensional movement control using electrocorticographic signals in humans. J Neural Eng 5(1):75–84. doi:10.1088/1741-2560/5/1/008

Schwartz AB, Moran DW (1999) Motor cortical activity during drawing movements: population representation during lemniscate tracing. J Neurophysiol 82(5):2705–2718

Schwartz AB, Kettner RE, Georgopoulos AP (1988) Primate motor cortex and free arm movements to visual targets in three-dimensional space. I. Relations between single cell discharge and direction of movement. J Neurosci 8(8):2913–2927

Schwartz AB, Cui XT, Weber DJ, Moran DW (2006) Brain-controlled interfaces: movement restoration with neural prosthetics. Neuron 52(1):205–220. doi:10.1016/j.neuron.2006.09.019

Serruya MD, Hatsopoulos NG, Paninski L, Fellows MR, Donoghue JP (2002) Instant neural control of a movement signal. Nature 416(6877):141–142

Taylor DM, Tillery SI, Schwartz AB (2002) Direct cortical control of 3D neuroprosthetic devices. Science 296(5574):1829–1832

Velliste M, Pere S, Spalding MC, Whitford AS, Schwartz AB (2008) Cortical control of a prosthetic arm for self-feeding. Nature 453:1098–1101. doi: 10.1038/nature06996

Wang W, Chan SS, Heldman DA, Moran DW (2007) Motor cortical representation of position and velocity during reaching. J Neurophysiol 97(6):4258–4270. doi:10.1152/jn.01180.2006

Wang W, Chan SS, Heldman DA, Moran DW (2010) Motor cortical representation of hand translation and rotation during reaching. J Neurosci 30(3):958–962. doi:10.1523/JNEUROSCI.3742-09.2010

Wisneski KJ, Anderson N, Schalk G, Smyth M, Moran D, Leuthardt EC (2008) Unique cortical physiology associated with ipsilateral hand movements and neuroprosthetic implications. Stroke 39(12):3351–3359. doi:10.1161/strokeaha.108.518175

Wolpaw JR, Birbaumer N (2005) Brain-computer interfaces for communication and control. Textbook of neural repair and rehabilitation. Cambridge University Press, Cambridge

Wolpaw JR, Birbaumer N, McFarland DJ, Pfurtscheller G, Vaughan TM (2002) Brain-computer interfaces for communication and control. Clin Neurophysiol 113(6):767–791